Hindawi
Advances in Materials Science and Engineering
Volume 2019, Article ID 6361032, 11 pages
https://doi.org/10.1155/2019/6361032

Research Article

Investigation of the Performance of the Ecofriendly Fiber-Reinforced Asphalt Mixture as a Sustainable Pavement Material

Bowen Guan,[1] Jianan Liu,[1] Jiayu Wu,[1] Jingyi Liu,[1] Haitao Tian,[1] Tengbin Huang,[1] Chengcheng Liu,[1] and Tao Ren[2]

[1]*School of Material Science and Engineering, Chang'an University, Xi'an, Shaanxi 710064, China*
[2]*The 2nd Engineering Co. Ltd. of China Railway 17 Bureau Group Corporation, Xi'an, Shaanxi 710064, China*

Correspondence should be addressed to Jianan Liu; liujn1996@163.com

Received 3 August 2019; Accepted 28 September 2019; Published 13 December 2019

Guest Editor: Andrea Grilli

This article presents a study to evaluate the performance of the ecofriendly calcium sulfate whisker fiber- (CSWF-) reinforced asphalt mixture as a sustainable pavement material. Asphalt mixtures containing 0.2 wt.%, 0.4 wt.%, 0.6 wt.%, and 0.8 wt.% of the CSWF were designed by the Marshall method. Asphalt mixtures without fiber were also prepared as control samples. The Marshall test, wheel-tracking test, low-temperature bending test, water sensitivity test, and fatigue test were conducted to evaluate the performance of the CSWF asphalt mixture. And the mechanism of fiber reinforcement was discussed. The results showed that the CSWF could improve the high-temperature stability and low-temperature crack resistance of the asphalt mixture. Water stability of asphalt mixtures in the presence of the CSWF was also improved. When the CSWF content was 0.4 wt.% of the total mixture, the performance of the asphalt mixture is the best. Compared with the conventional asphalt mixture, the CSWF asphalt mixture not only utilized power plant waste effectively to preserve ecosystems but also improved the performance of the pavement, which is suggested to be used in sustainable pavement construction and rehabilitation.

1. Introduction

Pavement plays a significant role in the transportation network affecting economic and social development of the country. At present, there are about billions of kilometers of pavement in the world [1]. These pavements enhance the social productivity and improve people's quality of life. However, pavement construction and rehabilitation consume a large number of materials derived from nonrenewable natural resources, which will destroy the environment. Meanwhile, due to the combined effects of repeated traffic loadings and the environment's influence such as rain, sunlight, and chemicals, the asphalt pavement begins to deteriorate significantly and needs to be rehabilitated after three to five years of service [2, 3]. Repeated rehabilitation of the pavement will also destroy the environment. Therefore, it is necessary to construct sustainable pavements. According to the definition of the Federal Highway Administration (FHWA), sustainable pavement should meet three requirements: meeting performance standards, utilizing resources effectively, and preserving the ecosystem [4]. A large number of studies have shown that the addition of ecofriendly fibers is an effective method to preserve ecosystems and improve the long-term performance of pavements [5–11]. In addition, some studies have found that green technologies hold promise in developing more sustainable pavements [1, 12]. Guan et al. found that the combination of 0.4 wt.% brucite fiber produced from the brucite tailings can effectively improve the strength and toughness of the fiber-reinforced asphalt mixture [13]. Nsengiyumva et al. found that the addition of the corn husk fiber could not only enhance the cracking resistance of HMA but also improve the cracking

resistance of cold-mix asphalt (CMA) [14]. Stempihar et al. found that fiber-reinforced asphalt concrete can be used as a sustainable paving material for airfields [15].

As a novel kind of ecofriendly fiber, the calcium sulfate whisker fiber (CSWF) is made from flue gas desulfurized gypsum which is the byproduct produced by limestone-gypsum wet flue gas desulfurization in thermal power plants [16]. The CSWF is widely used as a reinforced material and is also commonly applied to surface modification, polymer materials, papermaking technology, friction materials, and other aspects [17–21]. Yang et al. assessed the mechanical property of clay aerogel with the CSWF content, and the CSWF/clay aerogel composite was found to effectively form a dense "honeycomb" structure, increasing the modulus and consequently resulting in a high mechanical strength of composite materials [22]. Wang et al. evaluated the impact of the CSWF on the reinforced effect in silicone rubber composites and concluded that the CSWF was beneficial to the development of tensile strength and elongation of room-temperature-vulcanized silicone rubber/CSWF composites [23]. Xing et al. studied the effect and mechanism of the calcium carbonate whisker on the asphalt binder and found that the addition of the calcium carbonate whisker can improve the softening point of asphalt and decrease its penetration and ductility [24]. From these researches, it is found that, due to the high strength, large specific surface area, and high-temperature resistance, the CSWF can improve the performance of the matrix material effectively. The performance of the asphalt mixture may be improved by the addition of the CSWF. However, few studies reported this. In China, the deposit of flue gas desulfurization gypsum is up to billions of tons and amounts up to more than 50 million tons per year [25]. To utilize this power plant waste effectively and improve the performance of the pavement, the utilization of the CSWF in the asphalt mixture as a sustainable pavement material in the asphalt pavement may be a promising way.

In this paper, the performance of the ecofriendly CSWF-reinforced asphalt mixture as a sustainable pavement material was investigated. The performance of the CSWF asphalt mixture was evaluated by the Marshall test, wheel-tracking test, three-point bending test, fatigue test, and water sensitivity test under harsh environment. According to the test results above, the optimum content of the CSWF in the asphalt mixture was determined to satisfy the optimum performance of the asphalt mixture. Meanwhile, the mechanism of the CSWF-modified asphalt mixture was also discussed.

2. Materials and Methods

2.1. Materials. In this study, base asphalt 90# according to the American Society of Testing Materials (ASTM) was used as the binder. Its properties are shown in Table 1. Physical properties of the calcium sulfate whisker fiber are provided by the manufacturer, which are shown in Table 2. It can be seen from Table 2 that the calcium sulfate whisker has good thermal stability and high tensile strength. The morphology of the CSWF was captured by using an SEM. Figure 1(a) presents the appearance of the CSWF. And Figures 1(b), 1(c), and 1(d) show the micrograph of the CSWF at various scales from 50 μm to 5 μm. The CSWF exhibited a white fluffy powdery appearance with obvious edges and corners on the surface that promotes mixture resistance to several pavement distresses. Industrial sodium sulfate (Na_2SO_4) was used in the test, and the content of sodium sulfate was more than 99%. SK-90# matrix asphalt is used in this paper, and the coarse aggregate is the crushed basalt mineral, with a density of 2.86 g/cm^3. The fine aggregate was obtained from crushed basalt and mechanical sand, with a density of 2.83 g/cm^3. The mineral filler is of limestone type, with a density of 2.73 g/cm^3. And more than 95% of the filling size is less than 75 μm.

Table 1: Technical indicators of the asphalt binder.

Test properties	Unit	Test results	Test basis
Penetration (25°C, 100 g, 5 s)	0.1 mm	86.4	ASTM D5-97
Softening point	°C	47.0	ASTM D36-06
Ductility (15°C, 5 cm/min)	cm	182	ASTM D113-99
Wax content	%	1.74	ASTM D3344-90
Specific gravity	—	1.030	ASTM D70-76
Flash point	°C	304	ASTM D92-02
RTFOT (163°C, 75 min)			
Mass change	%	0.15	ASTM D2872-04
Penetration ratio (25°C)	%	60.5	ASTM D5-97
Ductility (10°C)	cm	10.1	ASTM D113-99

Table 2: Main characteristics of the CSWF.

Characteristics	Unit	Test results
Diameter	μm	2–4
Length	μm	40–60
Length/diameter ratio (mean)	—	16
Tensile strength	MPa	2050
Melt temperature	°C	1450

2.2. Sample Preparation. Gradation is the AC-13 asphalt mixture, and the designed gradation is shown in Table 3. The samples of the asphalt mixture with 0%, 0.2%, 0.4%, 0.6%, and 0.8% CSWF contents were prepared in accordance with the Chinese standard JTG E20-2011 [24]. To achieve good fiber dispersion, the CSWF and aggregate were mixed in a rotary mixer at 600 RPM for 90 seconds before the asphalt and mineral filler were added.

2.3. Scanning Electron Microscopy (SEM) Analyses. The microstructures of the CSWF and CSWF-reinforced asphalt mixture were examined by a scanning electron microscope (SEM).

2.4. Marshall Test. According to the content of different CSWFs, the optimum asphalt content (OAC), bulk specific gravity, air void volume (VV), voids in mineral aggregates (VMA), and Marshall stability (MS) of different asphalt mixtures were obtained by the Marshall test. All tests were

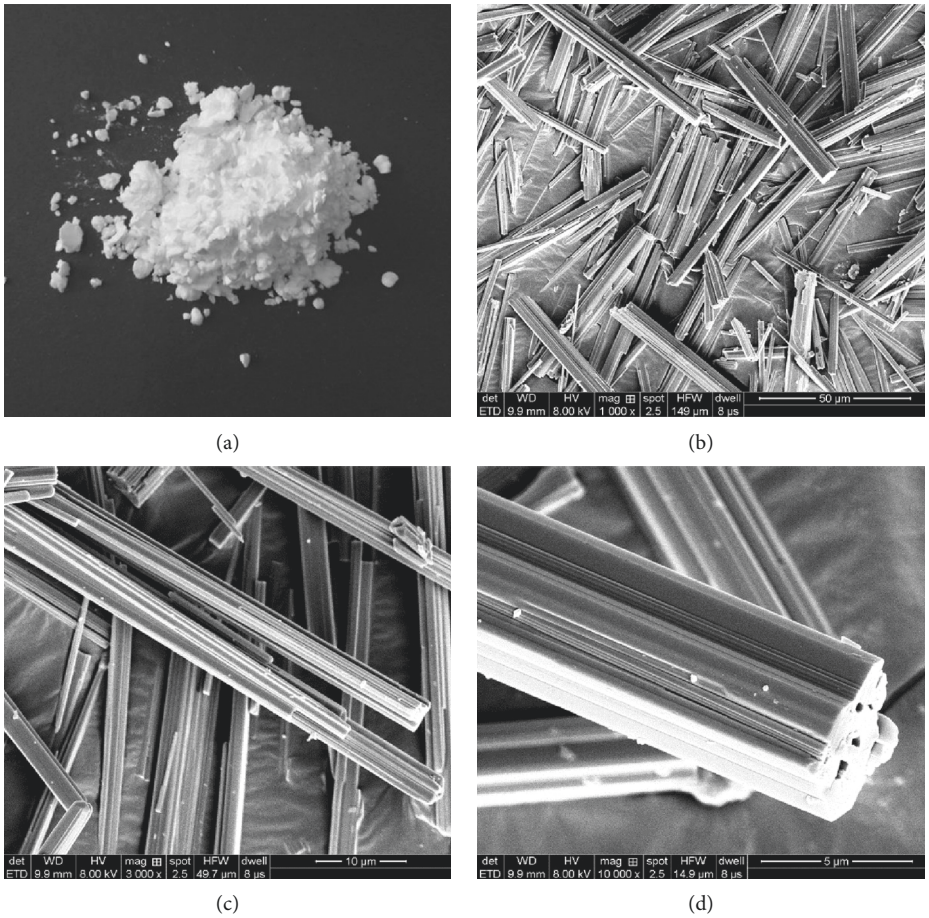

Figure 1: SEM micrographs of the CSWF: (a) appearance; (b) magnification: 1000 times; (c) magnification: 3000 times; (d) magnification: 10000 times.

Table 3: Mineral gradation of AC-13 mixture design.

Percent of aggregate passing for a given sieve size										
Sieve size (mm)	16	13.2	9.5	4.75	2.36	1.18	0.6	0.3	0.15	0.075
Percent passing	100	96	77	49.8	35	25	22	14	11	7

conducted following the method T0709 in JTG E20-2011 [23].

2.5. Wheel-Tracking Test. The wheel-tracking test was conducted in terms of JTG E20-2011 (T0719) [26]. The loose asphalt mixture was compacted into a few 300 × 300 × 50 mm slabs. These slabs were placed in the testing chamber at 60°C for 6 h. Then, a solid rubber tire moved back and forward on the slab surface with the travel distance of 230 ± 10 mm. The test load was 0.7 MPa, and the test wheel-rolling speed was 42 ± 1 cycles/min. The DS (times/mm) can be calculated by equation (1). Each asphalt mixture with different CSWF contents was repeatedly tested four times to acquire a reliable measure of the DS of the test specimen.

$$\mathrm{DS} = \frac{(t_2 - t_1) \times N}{d_2 - d_1} \times C_1 \times C_2 = \frac{42 \times 15}{d_{60} - d_{45}}, \qquad (1)$$

where t_1 and t_2 are time corresponding to 45 min and 60 min, respectively; N is the wheel-traveling speed, and $N = 42$ cycles/min in this paper; d_1 and d_2 are the rutting depth recorded at t_1 and t_2, respectively; and C_1 and C_2 are parameters and taken as 1 in this paper.

2.6. Low-Temperature Cracking Test. The three-point bending test was conducted in accordance with the Chinese standard JTG E20-2011 (T0715) [26] to evaluate the effect of the CSWF on the low-temperature cracking performance of the asphalt mixture. The span length was 200 mm. The midpoint of the beam was stressed, and the load was applied at a speed of 50 mm/min. The loose asphalt mixture was compacted into a 300 × 300 × 50 mm slab and sawed into a beam (250 × 30 × 35 mm) such that each span length is 200 mm. The test temperature was −10°C. Five parallel samples were used in this test.

$$R_B = \frac{3 \times L \times P_B}{2 \times b \times h^2},$$
$$\varepsilon_B = \frac{6 \times h \times d}{L^2}, \quad (2)$$
$$\varepsilon_B = \frac{6 \times h \times d}{L^2},$$

where R_B is the maximum bending stress (MPa); ε_B is the flexural strain ($\mu\varepsilon$); b is the width of the cross section (mm); h is the height of the cross section (mm); d is the midspan deflection at failure (mm); L is the span of the beam (mm); and P_B is the maximum load (N).

2.7. Freeze-Thaw Split Test. The freeze-thaw split test was conducted in accordance with the Chinese standard JTG E20-2011 (T0729) [26] to evaluate the effect of the CSWF-reinforced asphalt mixture on the water sensitivity performance. Marshall specimens were divided into two groups. The control group tested the splitting strength at 25°C with a loading rate of 50 mm/min, marked as R_{T1}. The second group tested the splitting strength under freeze-thaw cycles at a temperature between −18°C (16 h) and 60°C (24 h), marked as R_{T2}. Both conditioned and unconditioned specimens were put in a water bath at 25°C for at least 2 h. Finally, the specimens were loaded until failure, and the tensile strength ratio (TSR) was calculated using equations (3)–(5). Five parallel samples were used in this test.

$$R_{T1} = \frac{0.006287 P_{T1}}{h_1}, \quad (3)$$

$$R_{T2} = \frac{0.006287 P_{T2}}{h_2}, \quad (4)$$

$$\text{TSR} = \frac{\overline{R}_{T2}}{\overline{R}_{T1}} \times 100, \quad (5)$$

where TSR is the tensile strength ratio (%); R_{T1} is the average tensile strength (MPa) of the unconditioned specimen; R_{T2} is the average tensile strength (MPa) of the conditioned specimen; P_{T1} is the maximum value of the test load for the test pieces in the first group (N); and P_{T2} is the maximum value of the test load for the test pieces in the second group (N).

2.8. Four-Point Bending Fatigue Test. The fatigue life of the asphalt mixture was measured by a four-point bending fatigue test in JTG E20-2011(T0739) [26]. The four-point bending fatigue test is loaded in a partial sinusoidal loading with load-to-stress ratios of 0.1, 0.2, 0.3, and 0.4. The loose asphalt mixture was rolled into a square billet with a size of 400 × 300 × 75 mm and sawed into a beam (380 × 50 × 63 mm) at 25°C. Five parallel samples were used in this test.

2.9. Vacuum Immersion Attack Test. The vacuum immersion attack test of 10% (by weight of the total solution) sulfate concentration was improved by referring to the Chinese standard JTG E20-2011 (T0709-2011) [26]. The effect of sulfate attack on the CSWF-reinforced asphalt mixture was simulated by soaking Marshall specimens in 10% sodium sulfate solution. The Marshall stability of the control asphalt mixture and CSWF-reinforced asphalt mixture was tested. The specimens were put into a vacuum dryer with vacuum about 97.3 kPa for 15 min. Then, under the action of negative pressure, the sodium sulfate solution with a mass fraction of 10% was put into the dryer and all specimens were immersed in the sodium sulfate solution (the submergence height was no less than 20 mm). After 15 min, normal pressure was restored. Marshall specimens of the CSWF-reinforced asphalt mixture and Marshall specimens of the control asphalt mixture were tested for Marshall stability every 24 h after 48 h of immersion in sodium sulfate solution. The effect of water sensitivity of the CSWF-reinforced asphalt mixture under sulfate attack was studied, and the feasibility of using the CSWF-reinforced asphalt mixture in the sulfate environment was discussed. Three parallel samples were used in this test.

2.10. Sulfate-Freeze-Thaw Cycle Test. Marshall specimens (24 specimens) were formed by compaction (50 times for each side) with 0.4 wt.% CSWF, which were divided into 6 groups with 4 samples in each group. Referring to the freeze-thaw split test, the specimens were soaked for 10 h in 10% sodium sulfate instead of water. Marshall specimens without freeze-thaw cycle were tested for splitting tensile strength after 72 h of curing. The other five groups were first placed in a plastic bag containing 10% sodium sulfate solution and kept at −18°C for 16 h. Then, they were removed from the bag and immersed in a water bath at 60°C for 6 h. Five groups of specimens and control group were immersed in a water bath at 25°C for 2 h and tested. The 24 Marshall specimens were subjected to 0–5 freeze-thaw cycles, respectively, and the appearance changes of samples after freeze-thaw cycles were observed. Through the above experiments, the influence of salt-freeze-thaw cycle coupling on the water stability of the common asphalt mixture and CSWF-reinforced asphalt mixture was studied. Four parallel samples were used in this test.

2.11. Sulfate-Wet-Dry Cycle Test. The sulfate-wet-dry cycle was similar to the sulfate-freeze-thaw cycle. The Marshall specimens were immersed in 10% sodium sulfate solution and kept at 30°C for 12 h and oven-dried at 40°C for 12 h. After each sulfate-wet-dry cycle, four specimens were taken out to test the splitting strength, and the relevant test results were recorded. According to the results, the durability of the CSWF-reinforced asphalt mixture under sulfate-wet-dry cycles was analyzed. Three parallel samples were used in this test.

3. Results and Discussion

3.1. Marshall Index. Figures 2 to 6 show CSWF-reinforced asphalt mixture parameters, including the optimum asphalt content (OAC), bulk specific gravity, VV, VMA, and

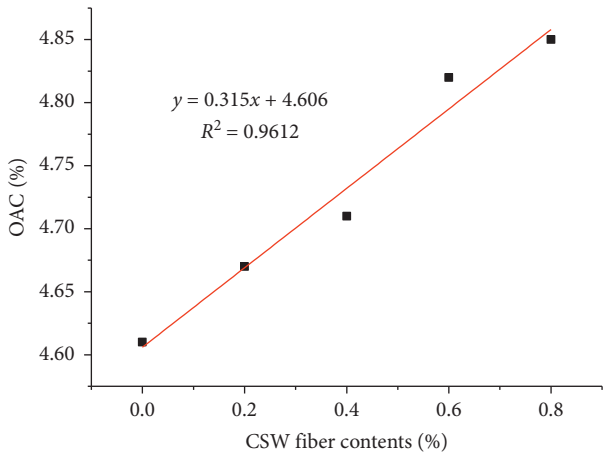

Figure 2: Change in the OAC for different CSWF contents.

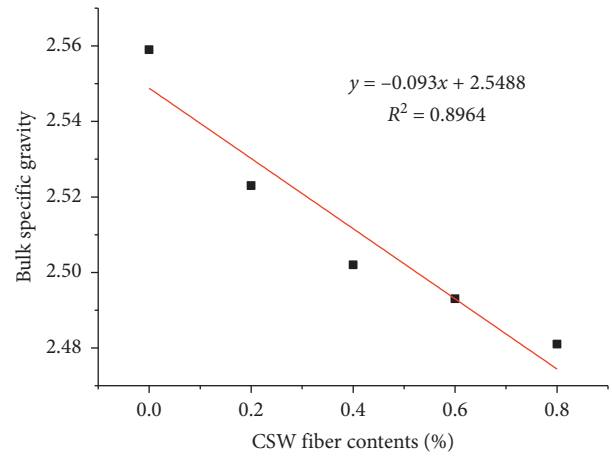

Figure 3: Change in bulk specific gravity for different CSWF contents.

Marshall stability (MS) of each mixture. With the CSWF content increase, the OAC increased from 4.61% to 4.85%. The main reason for this phenomenon was that the fiber increased the internal specific surface area and absorbed part of the free asphalt, so the asphalt content of the mixture increased.

Figure 3 shows the bulk specific gravity of the asphalt mixture with different CSWF contents. All of the bulk specific gravity values were between 2.48 and 2.56. With the CSWF content increase, the bulk specific gravity of the CSWF-reinforced asphalt mixture gradually decreased.

Figure 4 shows that the value of VV increased with the increase of the CSWF content. The data show a positive correlation between VV and CSWF content. This increase occurred probably due to the increase of CSWF surface area that absorbed more free asphalt.

Figure 5 reveals that, for different asphalt mixtures, the VMA also increase with the increasing content of the CSWF.

MS results are shown in Figure 6. Compared to those of the control group, the MS results of the test groups were improved by almost 7.4%, 21.7%, 16.2%, and 8.5%. Generally, the MS is an indicator to evaluate the anticracking ability. A larger MS value means a better anticracking ability. Maximum MS values were obtained when 0.40 wt.% CSWF was added.

3.2. High-Temperature Stability. Figure 7 displays the dynamic stability of the fiber-reinforced asphalt mixture with different CSWF contents. Ordinarily, a higher DS value means a preferable antirutting performance. When the CSWF content is less than 0.8 wt.%, the DS of the asphalt mixture with the CSWF goes up significantly, indicating that the high-temperature stability of the asphalt mixture can be improved. From Figure 7, it can be seen that dynamic stability of the asphalt mixture increased with the increase of the CSWF content. Compared with that of the nonfiber asphalt mixture, dynamic stability of the 0.4 wt.% content of the CSWF-reinforced asphalt mixture increased by 45.3%. Because the fiber absorbs the asphalt, the free asphalt content was reduced and the bonding strength was increased.

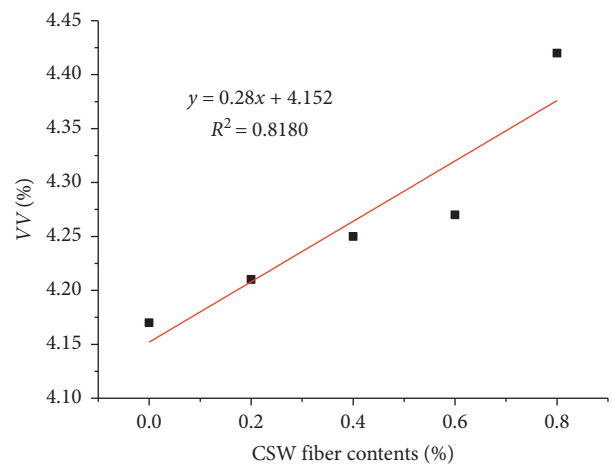

Figure 4: Change in VV for different CSWF contents.

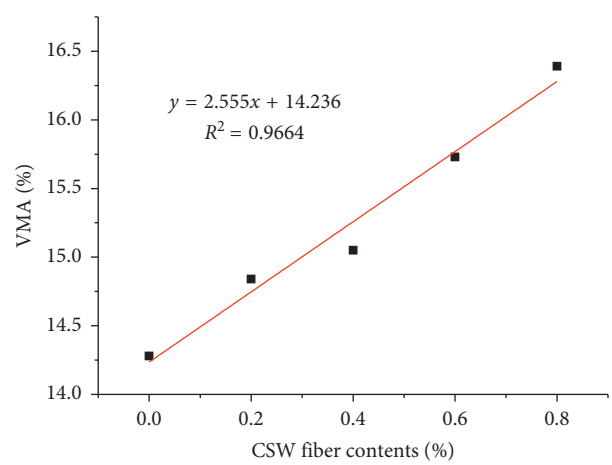

Figure 5: Change in VMA for different CSWF contents.

Figure 8 shows the micrograph of CSWF-reinforced asphalt. The fibers are evenly dispersed throughout the asphalt, increasing its mechanical strength. It is indicated that the

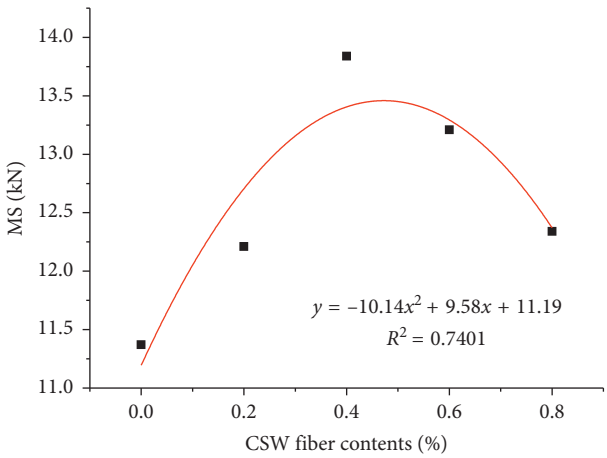

Figure 6: Change in MS for different CSWF contents.

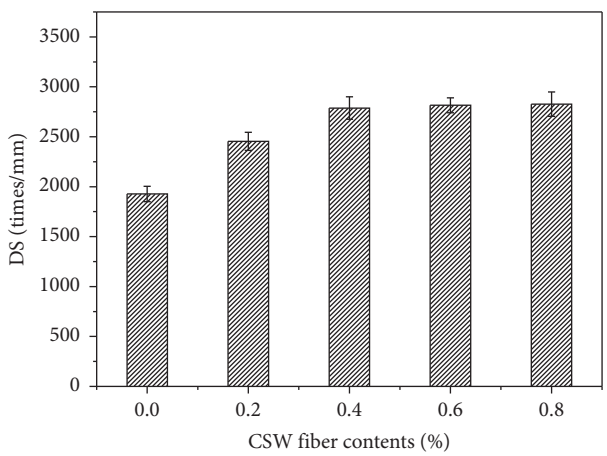

Figure 7: Change in DS for different CSWF contents.

CSWF formed a mesh structure in the asphalt mixture, with asphalt and CSWF having a good absorption and adhesion ability. In addition, the CSWF has the function of bridge connections, which could strengthen the weak area of the interface between the aggregate and the asphalt.

3.3. Low-Temperature Stability. The low-temperature bending test was conducted under −10°C. The result is elaborated in Figures 9–11. From Figures 9–11, it can be summarized that there is good parabolic curve fitting among the fiber-reinforced asphalt mixtures with different CSWF contents and the bending tensile strength, the maximum tensile strain, and the bending stiffness modulus. The bending tensile strength and tensile strain rose first and then came down with the CSWF content increase. It is indicated that the excessive content of the fiber would result in poor low-temperature stability of the asphalt mixture due to its uneven dispersion. Therefore, when the content of the CSWF reached a certain figure, the resistance of the mixture to the low-temperature crack will decrease. Furthermore, the bending tensile strength and tensile strain showed good performance at 0.4 wt.% CSWF content. The decrease of the bending stiffness modulus indicated that the CSWF could improve toughness and strong crack resistance of the asphalt mixture at low temperatures. Compared with that of the control asphalt mixture, the anticracking ability at low temperatures of the 0.4 wt.% content of the CSWF-reinforced asphalt mixture increased by 17.0%. The reason for this phenomenon is also attributed to the morphology effect of the CSWF with its needle-like granules. In addition, the CSWF has the function of bridge connections, which strengthens the weak area of the interface between the aggregate and the asphalt. The main reason for the above phenomenon is that the CSWF forms a special layered structure between the aggregate and the asphalt, which plays a key role in bridge connection and enhances the bonding effect with aggregates. Under the action of fibers, asphalt has higher stress recovery and ductility recovery, so as to improve the self-healing ability of the asphalt mixture [27, 28].

3.4. Water Sensitivity. Figure 12 shows the results of water sensitivity for five different types of asphalt mixtures. As shown in Figure 12, the freeze-thaw split strength of the CSWF-reinforced asphalt mixture increases from 0.2 wt.% to 0.8 wt.% compared to that of the control asphalt mixture. CSWF can improve the splitting tensile strength and water sensitivity of the asphalt mixture before and after freeze-thaw cycling. When the CSWF content is less than 0.4 wt.%, the splitting tensile strength significantly increased. From Figure 12, it is obvious to see that when the whisker content is about 0.4 wt.%, the tensile strength ratio of the freeze-thaw split is highest and then declines as the CSWF content increases. It is indicated that the optimum content of the CSWF was 0.4 wt.%. At the optimum content, the freeze-thaw splitting tensile strength of the CSWF-reinforced asphalt mixture increased by 12% and 28% compared with that of the control asphalt mixture and asphalt mixture without whisker addition after freeze-thaw cycles, respectively. The main reason for this phenomenon is that the fiber absorbed and assimilated on bitumen. During the freeze-thaw cycle, the CSWF increased the roughness of the interface that made the asphalt film thick and enhanced the interface bonding ability. This is the reason why the CSWF-reinforced asphalt mixture exhibited higher values for TSR and had good resistance to water damage.

3.5. Fatigue Performance Evaluation. Fatigue tests were carried out on the asphalt mixture mixed with and without CSWF. At the same stress ratio, the fatigue frequency and increase range of the asphalt mixture with the CSWF were calculated. The test data and results are shown in Figure 13. It can be seen from Figure 13 that, under the same stress ratio loading, the fatigue times of the asphalt mixture with the CSWF are all higher than those without CSWF. When the stress ratio was 0.1, the fatigue life of the CSWF-reinforced asphalt mixture increased by 7.2%, and when the stress ratio was 0.3, the fatigue life increased by 54.2%. These data show that the effect of CSWF addition on the fatigue frequency of the asphalt mixture was not obvious when the stress level was low. With the increase of stress ratio, the

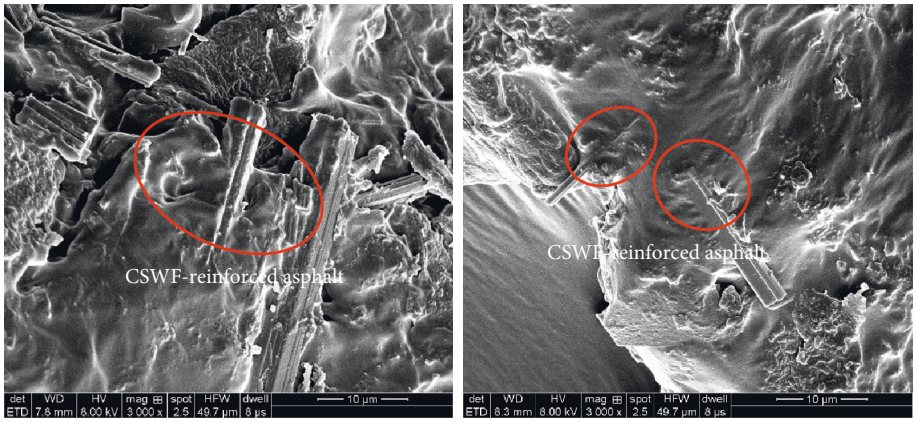

Figure 8: SEM micrographs of CSWF-reinforced asphalt.

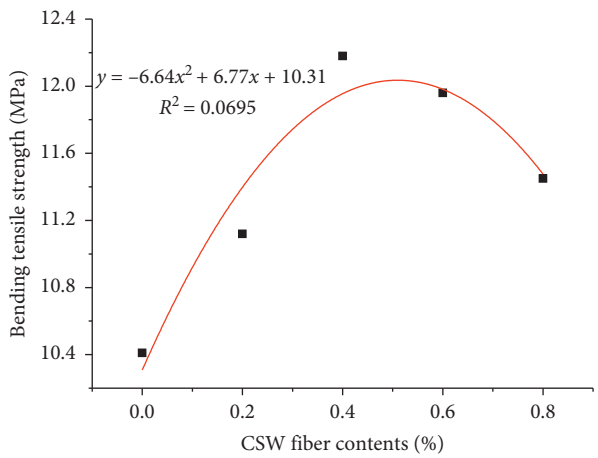

Figure 9: Bending tensile strength for different CSWF contents.

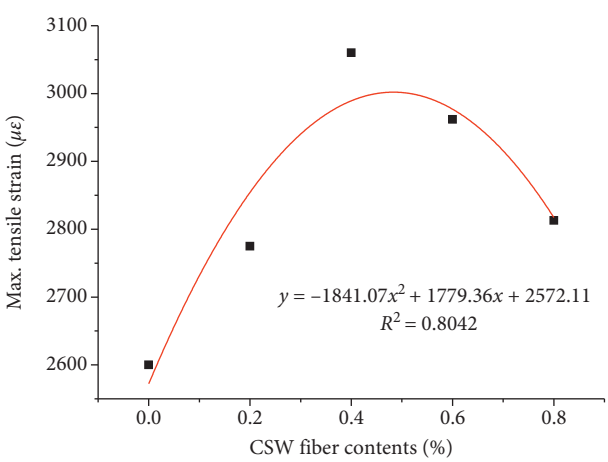

Figure 10: Maximum tensile strain for different CSWF contents.

CSWF improved the fatigue resistance of the asphalt mixture significantly, and the fatigue life of the fiber-modified asphalt mixture had been greatly improved. The addition of the CSWF could improve the fatigue life of the asphalt mixture and the fiber-modified asphalt mixture under the constantly changing stress state as well as extend the service life of the asphalt mixture.

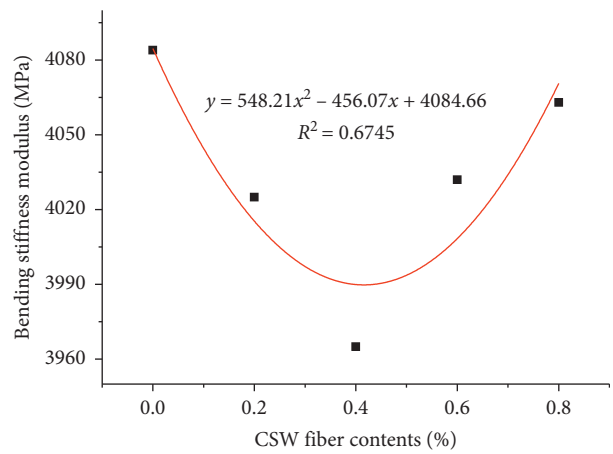

Figure 11: Bending stiffness modulus for different CSWF contents.

3.6. Water Sensitivity in Sulfate Environment. MS test results of various asphalt mixtures after sulfate attack are shown in Figure 14. After 48 h immersion in the Marshall test, the Marshall stability of the control sample was 10.47 kN and that of the CSWF-reinforced asphalt mixture was 10.58 kN. The MS of the control sample decreased 19.5% and 51.6% when soaked in sodium sulfate for 2 d and 8 d compared with 2 d immersion in water, respectively. However, the MS of the CSWF-reinforced asphalt mixture decreased 17.7% and 40.9% in 2 d and 8 d under sulfate attack compared with 2 d immersion in water, respectively. It is indicated that the performance of the asphalt mixture in the salt attack environment declined more seriously than that in the water environment, and the CSWF has certain enhancement effect on sulfate attack resistance of the asphalt mixture. And the CSWF can enhance the anti-sulfate attack ability of the asphalt mixture.

3.7. Water Sensitivity under Salt-Freeze-Thaw Cycles. The test data of freeze-thaw splitting tensile strength and freeze-thaw splitting tensile strength ratio without freeze-thaw cycles and each freeze-thaw cycle are shown in Figure 15. It can be seen that, under the action of salt-freeze-thaw cycles, the tensile strength of freeze-thaw cracking of the two mixtures

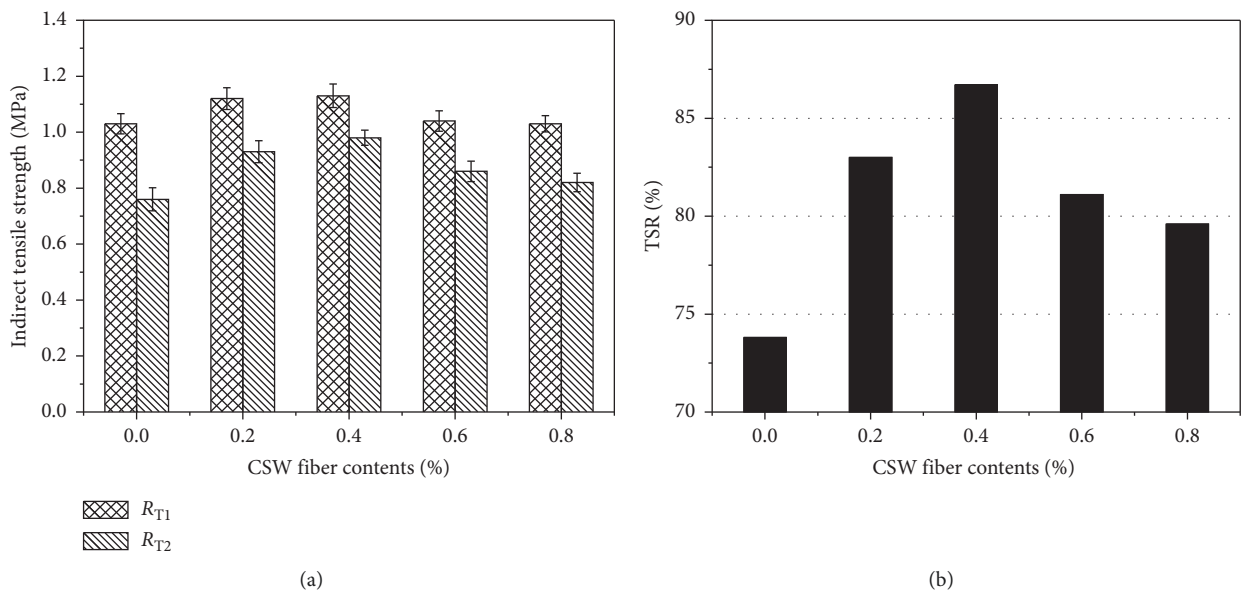

Figure 12: Water sensitivity of different CSWF contents: (a) residual strength; (b) TSR.

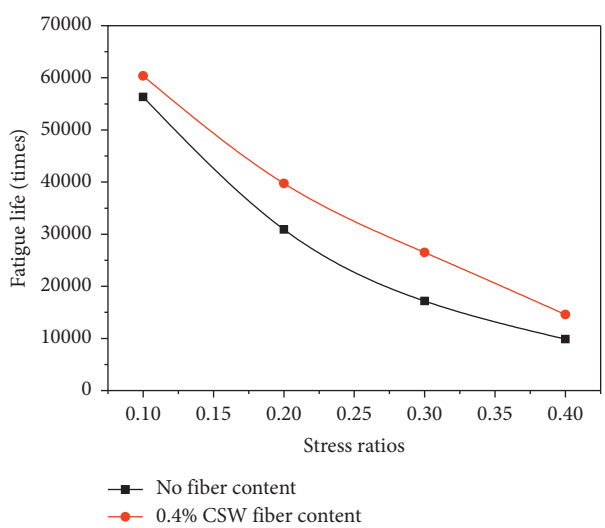

Figure 13: Fatigue life of the mixture under different stress ratios.

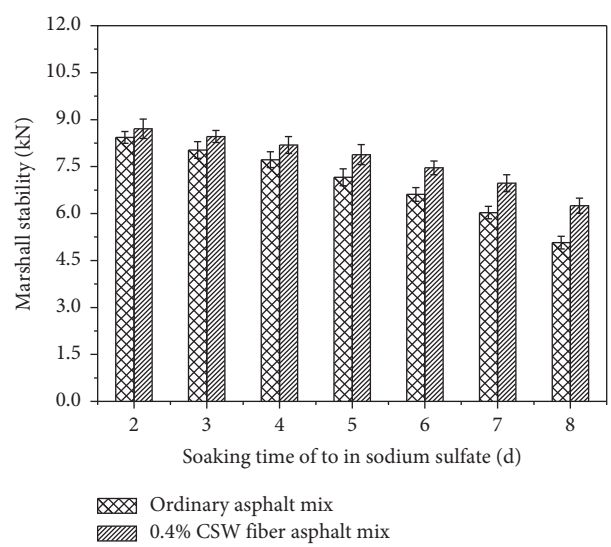

Figure 14: Marshall stability of the mix under the sodium sulfate solution attack.

decreased significantly. After 5 salt-freeze-thaw cycles, the tensile strength of freeze-thaw splitting of the ordinary asphalt mixture decreased to 0.30 MPa, and tensile strength of the 0.4 wt.% content of the CSWF-reinforced asphalt mixture also went down to 0.47 MPa. The tensile strength ratios of freeze-thaw cracking were 27% and 39.8%, respectively. It is indicated that the addition of the CSWF could effectively improve the sulfate attack resistance and freeze-thaw cycle resistance of the asphalt mixture.

3.8. Water Sensitivity under Salt-Wet-Dry Cycles. It can be seen from Figure 16 that the splitting strength of both mixtures decreased under the continuous action of the salt-wet-dry cycle. The addition of the CSWF could improve the sulfate attack resistance and wet-dry cycle resistance of the asphalt mixture. This is similar to what happens in the salt-freeze-thaw cycle, but not as intense as in that cycle.

3.9. Comparison with Different Fiber-Reinforced Asphalt Mixtures. Table 4 shows physical properties of different fibers. Table 5 shows the results of high-temperature stability, low-temperature stability, water sensitivity, and fatigue performance under different types and the optimum content of the fiber. Compared with that of the control group, the DS of 0.4 wt.% CSWF-reinforced asphalt mixture increased by 44.6%, the low-temperature crack resistance increased by 17%, and the TSR increased by 17.4%. As can be seen from Table 5, compared with that of other fiber-reinforced asphalt mixtures, the road performance of the

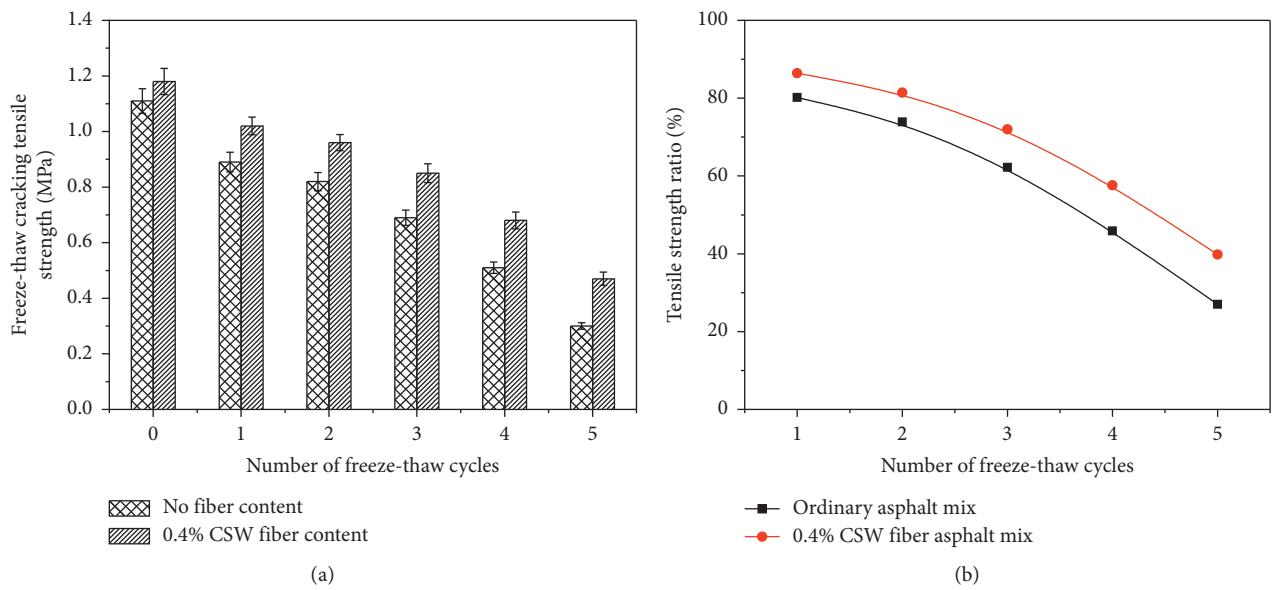

Figure 15: Variation curves of tensile strength ratio of freeze-thaw cracking with the number of sulfate-freeze-thaw cycles: (a) tensile strength of freeze-thaw cracking; (b) tensile strength ratio of freeze-thaw cracking.

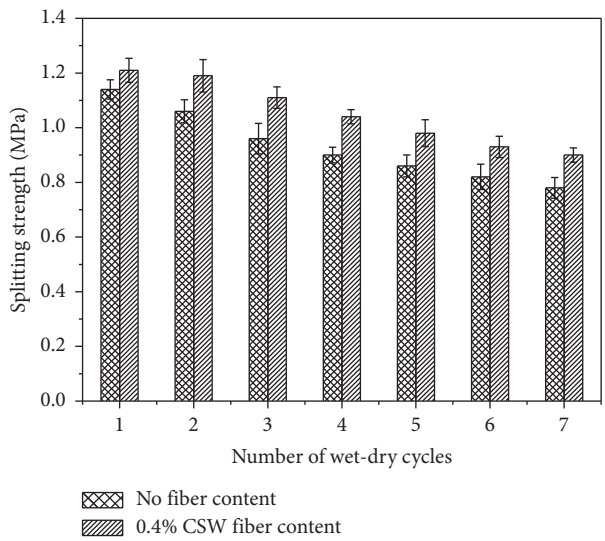

Figure 16: Variation curves of splitting strength with the number of sulfate-wet-dry cycles.

Table 4: Physical properties of different fibers.

Fiber type	Properties					Reference
	Diameter (mm)	Length (mm)	Length/diameter ratio	Tensile strength (MPa)	Melt temperature (°C)	
CSWF	0.003	0.05	16	2050	>1400	This paper
Brucite fiber	0.02	0.5	25	932	>400	[13]
Lignin fiber	0.045	1.1	24	—	—	[29]
Glass fiber	12	—	—	3250	>1500	[30]
Basalt fiber	0.013	6	460	3200	—	[8]
Polyester fiber	0.02	6	300	531	—	[29]
Polyacrylonitrile fiber	0.013	5	385	>910	—	[29]

Table 5: Improvement of asphalt mixture performance by addition of different fibers.

Types of fibers	Optimum fiber content (%)	Improvement of asphalt mixture performance						Reference
		Dynamic stability (times/mm)	Max. bending stress (MPa) (%)	Max. tensile strain ($\mu\varepsilon$) (%)	TSR (%)	Fatigue life		
						Stress ratio	Number of fatigue life cycles (%)	
CSWF	0.4	+44.16	+17.0	+13.9%	86.7	0.3	+54.2%	This paper
Brucite fiber	0.4	+53.8	+23.4	+13.0%	87.5	0.3	+18.3%	[13]
Lignin fiber	0.35	+8.4	+11.7	+6.0%	68.0	0.3	+68.1%	[29]
Diatomite + glass fiber	0.2 + 0.3	+77.4	+9.6	+26.2%	—	0.4	+114.3%	[30]
Basalt fiber	0.4	+82.5	+22.5	—	93.0	—	—	[8]
Polyester fiber	0.35	+19.5	+8.1	+4.0%	77.5	0.3	+59.8%	[29]
Polyacrylonitrile fiber	0.35	+32.5	+6.4	+2.0%	75.5	0.3	+130.0%	[29]

CSWF-reinforced asphalt mixture is not significantly improved, but the enhancement effect is relatively balanced. As can be seen from Figure 5, the CSWF is a single crystal fiber which has a small diameter and length compared with other fibers but has a high tensile strength. The efficiency of a fiber-reinforced composite depends on the fiber/matrix interface stress transfer capability. Because of the small particle size of the CSWF, the mechanical property enhancement effect of the asphalt mixture is poor. However, under various harsh environments, the CSWF with needle-like granules and small particle size forms embedding and anchoring in the mixture, consequently increasing the mechanical bonding force between the asphalt and the aggregate.

4. Conclusions

This study investigated the performance of the ecofriendly calcium sulfate whisker fiber- (CSWF-) reinforced asphalt mixture as a sustainable pavement material. Conclusions were summarized as follows:

(1) With the increase of the CSWF content, the anti-rutting performance, low-temperature crack resistance, and durability of the asphalt mixture were improved significantly.

(2) According to the analysis of road performance results, the optimal content of the CSWF is 0.4 wt.%. Under the 0.4 wt.% content of the CSWF, DS, bending tensile strength, and TSR increased by 44.6%, 17.0%, and 17.4% compared with those of the control sample, respectively.

(3) Durability damage of the asphalt mixture is caused by infiltration and expansion pressure generated in the process of sulfate crystallization-dissolution. The CSWF-reinforced asphalt mixture has better resistance to cracking strength degradation under the coupling action of salt-freeze-thaw cycles and salt-dry-wet cycles.

(4) Compared with the conventional asphalt mixture, the CSWF asphalt mixture not only utilized power plant waste effectively to preserve ecosystems but also improved the performance of the pavement, which is suggested to be used in sustainable pavement construction and rehabilitation.

Data Availability

The data used to support the findings of this study are included within the article.

Conflicts of Interest

The authors declare that they have no conflicts of interest.

Acknowledgments

The authors wish to thank the financial support from the Program of China Scholarships Council (No. 201806565048), the Program of Traffic Innovation Management Consulting Research Project of Yunnan Province (No. 2019304), the China Postdoctoral Science Foundation (No. 2019M653520), the Natural Science Foundation of Jiangxi Province (20192BBG70064), and the Fundamental Research Funds for the Central Universities, CHD (Nos. 300102319102, 300102319202, and 3001102319501).

References

[1] W. J. Sun, G. Lu, C. Ye et al., "The state of the art: application of green technology in sustainable pavement," *Advances in Materials Science and Engineering*, vol. 2018, Article ID 9760464, 19 pages, 2018.

[2] D. V. Thanh and C. P. Feng, "Study on Marshall and Rutting test of SMA at abnormally high temperature," *Construction and Building Materials*, vol. 47, pp. 1337–1341, 2013.

[3] S. Tayfur, H. Ozen, and A. Aksoy, "Investigation of rutting performance of asphalt mixtures containing polymer modifiers," *Construction and Building Materials*, vol. 21, no. 2, pp. 328–337, 2007.

[4] American Association of State Highway and Transportation Officials (AASHTO), *Transportation and Sustainability Best Practices Background, Sustainability Peer Exchange—Center for Environmental Excellence*, American Association of State Highway and Transportation Officials, Washington, DC, USA, 2009.

[5] H. K. Shanbara, F. Ruddock, and W. Atherton, "A laboratory study of high-performance cold mix asphalt mixtures reinforced with natural and synthetic fibres," *Construction and Building Materials*, vol. 172, pp. 166–175, 2018.

[6] Q. Xue, L. Liu, and Y. J. Chen, "Study on the action effect of pavement straw composite fiber material in asphalt mixture," *Construction and Building Materials*, vol. 43, pp. 293–299, 2013.

[7] T. Takaikaew, P. Tepsriha, S. Horpibulsuk, M. Hoy, K. E. Kaloush, and A. Arulrajah, "Performance of fiber-reinforced asphalt concretes with various asphalt binders in Thailand," *Journal of Materials in Civil Engineering*, vol. 30, no. 8, Article ID 04018193, 2018.

[8] Y. C. Cheng, W. Wang, Y. Gong, S. Wang, S. Yang, and X. Sun, "Comparative study on the damage characteristics of asphalt mixtures reinforced with an eco-friendly basalt fiber under freeze-thaw cycles," *Materials*, vol. 11, no. 12, p. 2488, 2018.

[9] O. S. Abiola, W. K. Kupolati, E. R. Sadiku, and J. M. Ndambuki, "Utilisation of natural fibre as modifier in bituminous mixes: a review," *Construction and Building Materials*, vol. 54, pp. 305–312, 2014.

[10] S. Serin, N. Morova, M. Saltan, and S. Terzi, "Investigation of usability of steel fibers in asphalt concrete mixtures," *Construction and Building Materials*, vol. 36, pp. 238–244, 2012.

[11] D. Luo, A. Khater, Y. Yue et al., "The performance of asphalt mixtures modified with lignin fiber and glass fiber: a review," *Construction and Building Materials*, vol. 209, pp. 377–387, 2019.

[12] R. He, X. Huang, J. Zhang, Y. Geng, and H. Guo, "Preparation and evaluation of exhaust-purifying cement concrete employing titanium dioxide," *Materials*, vol. 12, no. 13, p. 2182, 2019.

[13] B. W. Guan, R. Xiong, R. He, S. Chen, and D. Ding, "Investigation of usability of brucite fiber in asphalt mixture," *International Journal of Pavement Research and Technology*, vol. 7, no. 3, pp. 193–202, 2014.

[14] G. M. Nsengiyumva, K. Santosh, Y.-R. Kim, H. Xu, and Y. Yang, *New Mixture Additives for Sustainable Bituminous Pavements*, Nebraska Transportation Center, Lincoln, NE, USA, 2018.

[15] J. J. Stempihar, M. I. Souliman, and K. E. Kaloush, "Fiber-reinforced asphalt concrete as sustainable paving material for airfields transportation research record," *Journal of the Transportation Research Board*, vol. 2266, no. 1, pp. 60–68, 2012.

[16] X. Wang, L. Wang, Y. Wang et al., "Calcium sulfate hemihydrate whiskers obtained from flue gas desulfurization gypsum and used for the adsorption removal of lead," *Crystals*, vol. 7, no. 9, p. 270, 2017.

[17] H. Fan, X. Song, Y. Xu, and J. Yu, "Insights into the modification for improving the surface property of calcium sulfate whisker: experimental and DFT simulation study," *Applied Surface Science*, vol. 478, pp. 594–600, 2019.

[18] W. J. Yuan, J. Cui, Y. Cai, and S. Xu, "A novel surface modification for calcium sulfate whisker used for reinforcement of poly(vinyl chloride)," *Journal of Polymer Research*, vol. 22, no. 9, p. 173, 2015.

[19] X. Feng, Y. Zhang, G. Wang, M. Miao, and L. Shi, "Dual-surface modification of calcium sulfate whisker with sodium hexametaphosphate/silica and use as new water-resistant reinforcing fillers in papermaking," *Powder Technology*, vol. 271, pp. 1–6, 2015.

[20] W. Yuan, J. Cui, and S. Xu, "Mechanical properties and interfacial interaction of modified calcium sulfate whisker/poly(vinyl chloride) composites," *Journal of Materials Science & Technology*, vol. 32, no. 12, pp. 1352–1360, 2016.

[21] J. Wang, K. Yang, and S. Lu, "Preparation and characteristic of novel silicone rubber composites based on organophilic calcium sulfate whisker," *High Performance Polymers*, vol. 23, no. 2, pp. 141–150, 2011.

[22] L. Yang, Y. Lu, F. He, H. Wu, T. Xu, and M. Xiao, "Preparation and characterization of clay aerogel composites reinforced by calcium sulfate whisker," *Journal of Nanoscience and Nanotechnology*, vol. 18, no. 11, pp. 7896–7901, 2018.

[23] J. C. Wang, X. C. Pan, Y. Xue, and S. J. Cang, "Studies on the application properties of calcium sulfate whisker in silicone rubber composites," *Journal of Elastomers & Plastics*, vol. 44, no. 1, pp. 55–66, 2011.

[24] X. Y. Xing, J. Pei, R. Li, and X. Tan, "Effect and mechanism of calcium carbonate whisker on asphalt binde Materials," *Research Express*, vol. 6, no. 5, Article ID 055306, 2019.

[25] H. J. Sun, D. Tan, T. Peng, and Y. Liang, "Preparation of calcium sulfate whisker by atmospheric acidification method from flue gas desulfurization gypsum," *Procedia Environmental Sciences*, vol. 31, pp. 621–626, 2016.

[26] JTG E20-2011, *Standard Test Methods of Bitumen and Bituminous Mixtures for Highway Engineering*, China Communications Press, Beijing, China, 2011.

[27] B. A. Shu, S. Wu, L. Dong et al., "Synthesis and properties of microwave and crack responsive fibers encapsulating rejuvenator for bitumen self-healing," *Materials Research Express*, vol. 6, no. 8, Article ID 085306, 2019.

[28] B. A. Shu, S. Wu, L. Dong et al., "Microfluidic synthesis of polymeric fibers containing rejuvenating agent for asphalt self-healing," *Construction and Building Materials*, vol. 219, pp. 176–183, 2019.

[29] Q. Xu, H. Chen, and J. A. Prozzi, "Performance of fiber reinforced asphalt concrete under environmental temperature and water effects," *Construction and Building Materials*, vol. 24, no. 10, pp. 2003–2010, 2010.

[30] Q. L. Guo, L. Li, Y. Cheng, Y. Jiao, and C. Xu, "Laboratory evaluation on performance of diatomite and glass fiber compound modified asphalt mixture," *Materials & Design*, vol. 66, pp. 51–59, 2015.